

The nucleation, growth and stabilization of vortex lattices

A. A. Penckwitt and R. J. Ballagh

Department of Physics, University of Otago, Dunedin, New Zealand

C. W. Gardiner

School of Chemical and Physical Sciences, Victoria University, Wellington, New Zealand

We give a simple unified theory of vortex nucleation and vortex lattice formation which is valid from the initiation process up to the final stabilization of the lattice. We treat the growth of vortex lattices from a rotating thermal cloud, and their production using a rotating trap. We find results consistent with previous work on the critical velocity or critical angular velocity for vortex formation, and predict the initial number of vortices expected before their self assembly into a lattice. We show that the thermal cloud plays a crucial role in the process of vortex lattice nucleation.

PACS numbers: 03.75 Fi

The opportunity that Bose Einstein condensates present for precisely controlled experimental and theoretical study of superfluids has revived an intense interest in the properties and behavior of quantized vortices. Many different theoretical calculations have been made of stationary single vortex states and their excitations ([1] and references therein), and vortex lattices ([2] and references therein) in Bose condensates, but the recent experimental observations of vortex lattices [3, 4, 5, 6, 7, 8, 9] have focussed attention on the *mechanisms* of vortex formation.

One experimental method for creating vortices is to stir a condensate with an anisotropic potential, and a number of theoretical analyses of this scenario have been made in terms of the Gross-Pitaevskii equation, e.g. [10, 11, 12, 13]. The view of these treatments is that the perturber causes a mixing of the condensate ground state and excited condensate states (with angular momentum values determined by the stirrer geometry). Typically, a perturbative calculation is used to obtain a critical rotational speed (or a critical linear speed at the Thomas-Fermi radius) of the stirrer at which the mixing becomes effective. The argument is then made that an instability will lead to growth of the vortex state. A more complete non-perturbative calculation for a localized rotating stirrer [14] shows that in this case the mixing is predominantly between the ground state and an $l = 1$ vortex state, and that as the relative amplitudes evolve by coherent “Rabi cycling”, the full condensate exhibits a vortex cycling from infinity to the central regions of the condensate. No coherent mixing mechanisms, however, can explain the formation of a *vortex lattice*, since an energy barrier exists between the superposition state and the vortex lattice state, and some additional mechanism is required to remove the energy liberated when the vortex lattice is formed.

An alternative method of producing vortices, in which a vapor of cold atoms is evaporatively cooled so as to preserve its angular momentum has been demonstrated by Haljan *et al.* [5]. In this experiment, which involves no stirring potential, the mechanism of formation of the vortices must involve a modification of the theory of condensate growth (which now exists in a reasonably good quantitative form; [15] and ref-

erences therein) to take account of the non-zero angular momentum of the vapor from which the condensate is formed. In this paper we will show that the mechanism thus demonstrated is the fundamental process in those experiments in which the stirring of the condensate apparently generates a vortex lattice. Weak stirring, in the absence of any thermal cloud, only produces “Rabi cycling” of angular momentum in and out of the condensate. However, if the stirring also produces a rotating thermal cloud, then, by the same process responsible for the growth of a condensate [16], angular momentum is transferred *irreversibly* into the condensate, leading in equilibrium to a rotating vortex lattice. In general terms, this has already been noted in [17], and in [18] we derived a very simplified vortex growth equation—given below as Eq. (3)—embodying the essentials of this concept.

Other theoretical treatments of condensate dynamics at finite temperature have been applied to the case of vortex dynamics. Zhuravlev *et al.* [17] studied the interaction of vortex lattices with a thermal cloud in the presence of a trap asymmetry, and from broad conservation principles they obtained equations for the time evolution of the angular velocity of the condensate and thermal cloud, and the transfer of energy between them. Williams *et al.* [19] showed how the inclusion of interactions with a thermal vapor cloud would give rise to an instability of surface modes, as required to produce vortices. Our own treatment [18] had a basis broadly equivalent to that of Williams *et al.*, but showed how the interaction with the vapor cloud could produce an equation which should describe the full process of vortex nucleation, growth and stabilization. Using this equation, we will show in this paper how the growth of vortex lattices can be understood as a condensate growth process, and that the condition that the gain in this growth process be positive is the same as the criteria noted above for vortex nucleation. We also demonstrate explicitly how the vortices produced in the “Rabi cycling” caused by a rotating trap nucleate the growth process, which then proceeds to dominate the vortex lattice formation process.

The Gross-Pitaevskii equation for $\psi_R = \exp(i \Omega \cdot \mathbf{L} t / \hbar) \psi$, the condensate wavefunction in a frame of reference rotating

with angular velocity Ω , takes the form

$$i\hbar \frac{\partial \psi_R}{\partial t} = \left(-\frac{\hbar^2}{2m} \nabla^2 + V_T^R(\mathbf{x}) + u|\psi_R|^2 - \Omega \cdot \mathbf{L} \right) \psi_R, \quad (1)$$

where $V_T^R(\mathbf{x})$ is the trap potential in the rotating frame. A vortex lattice results from the stationary solutions of Eq. (1) satisfying $i\hbar \partial \psi_R / \partial t = \mu_C \psi_R$ [2, 20], which are normally obtained by integrating the Gross-Pitaevskii equation along an imaginary time direction [20]. Indeed, noting that the achievement of the vortex lattice stationary state requires dissipation in order to allow the system to settle into the energy minimum associated with the lattice, Tsubota *et al.* [21] proposed an *ad hoc* modification of this method as a phenomenological model of the process of vortex lattice formation. They modified the left-hand side of Eq. (1) to $(1 + i\gamma) i\hbar \partial \psi_R / \partial t$, and compensated for the consequent loss of probability by continuously adjusting the norm of the wavefunction.

Origin of dissipation: When the condensate is grown from a rotating vapor cloud the growth process itself is dissipative, and in the experiments of [3, 4, 5, 6] dissipation can arise by transfer of atoms between the thermal cloud and the condensate. The vortex growth equation derived in [18] uses quantum kinetic theory for the growth of the wavefunction for a condensate trapped in a potential $V_T(\mathbf{x}, t)$ rotating with angular velocity Ω , from a thermal cloud held at temperature T and chemical potential μ and rotating with angular velocity α . A dissipative term arises from collisions between atoms in a thermal cloud of atoms trapped by the same potential as the condensate, in which one of the colliding atoms enters the condensate after the collision. The net rate at which atoms enter and leave the condensate as the result of such collisions is characterized by a coefficient

$$W^+(\mathbf{x}) = \frac{u^2}{(2\pi)^5 \hbar^2} \int d^3 \mathbf{K}_1 d^3 \mathbf{K}_2 d^3 \mathbf{K}_3 \delta(\omega_{123}) \times \delta(\mathbf{K}_1 + \mathbf{K}_2 - \mathbf{K}_3) F_1 F_2 (1 + F_3) \quad (2a)$$

$$\approx g \times 4m(akT)^2 / \pi \hbar^3, \quad (2b)$$

and in practice $g \approx 3$ fits most growth experiments. Here $F(\mathbf{x}, \mathbf{K})$ is the Bose-Einstein distribution function for a thermal cloud in an effective potential in the frame rotating at the *cloud's* angular velocity α , i.e. $V_\alpha(\mathbf{x}) \equiv \bar{V}_T(\mathbf{x}) - m(\alpha \times \mathbf{x})^2 / 2$, where $\bar{V}_T(\mathbf{x})$ is the time averaged trap potential over the differential rotation between the trap and the cloud. The vortex growth equation takes the form in the frame rotating with the *trap potential*

$$i\hbar \frac{\partial \psi_R}{\partial t} = \left(-\frac{\hbar^2}{2m} \nabla^2 + V_T^R(\mathbf{x}) + u|\psi_R|^2 - \Omega \cdot \mathbf{L} \right) \psi_R + i\gamma \left(\mu + (\alpha - \Omega) \cdot \mathbf{L} - i\hbar \frac{\partial}{\partial t} \right) \psi_R, \quad (3)$$

where $\gamma \equiv \hbar W^+ / kT$. It is important to distinguish between the *cloud's* angular velocity α , and the *trap's* angular velocity Ω . If these are different the distribution of the thermal cloud

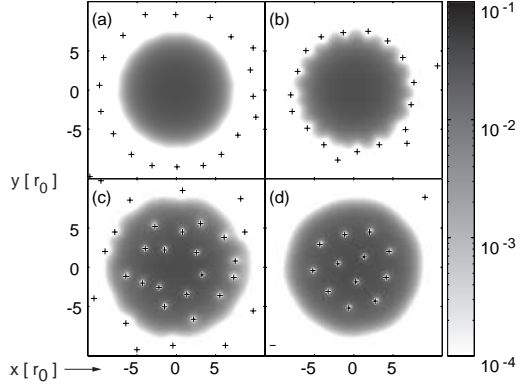


FIG. 1: Condensate density during formation of vortex lattice from a rotating thermal cloud. Vortices are marked by + or - according to their sense. (a) $t = 29.28 t_0$, (b) $t = 37.70 t_0$, (c) $t = 52.40 t_0$, (d) $t = 187.24 t_0$. Condensate wavefunction seeded as described in text. Parameters are $\alpha = 0.65 \omega$, $\mu = 12\hbar\omega$, $\gamma = 0.1$, $u = 1000u_0$, initial $\mu_C = 12.7\hbar\omega$. Units are: time $t_0 = 1/\omega$, distance $r_0 = \sqrt{\hbar/2m\omega}$, collisional strength $u_0 = \hbar\omega r_0^2$.

is not truly thermodynamic equilibrium, and the form chosen represents an approximation expressing the experimental observation that it is very difficult to spin up a thermal cloud by means of a rotating potential. One therefore expects that $\alpha < \Omega$. In this paper, however, we shall consider mainly the cases in which either the trap is cylindrically symmetric, so that we may set $\Omega = 0$, or in which the cloud and the trap rotate at the same velocity, so $\alpha = \Omega$. Eq. (3) is essentially equivalent in terms of the physical assumptions required for its derivation to that of [19], although its appearance is very different, and it is in practice easier to solve. In contrast, although Eq. (3) looks superficially very similar to that of [21], it is in fact very different, as explained in [18].

Simulation results for a rotating vapor cloud: We have simulated Eq. (3) in two dimensions for many different scenarios, and in Fig. 1 we present a time sequence of results from a representative case in which the condensate is initially in the ground state of a rotationally symmetric harmonic trap of frequency ω , the thermal cloud has $\mu = 12\hbar\omega$, and $\alpha = 0.65 \omega$. The initial condensate has unit norm and chemical potential $\mu_C = 12.7\hbar\omega$, although they can be any non-zero number. We simulate the non-stimulated collisions which start the process by adding to the initial wavefunction a uniform superposition of angular momentum states with $l = 1$ to 30, on a Gaussian radial profile centered at the Thomas-Fermi radius and with maximum amplitude $\sim 2 \times 10^{-7}$.

Fig. 1(a) is a density plot of the condensate near the end of the first stage of the evolution, in which an imperfect ring of 19 vortices arrives from infinity to just outside the Thomas-Fermi radius. As this ring shrinks further (Fig. 1(b)), several vortices are shed, and a dominant ring of 16 vortices passes through the Thomas-Fermi radius into the interior of the condensate. These vortices then distribute themselves irregularly but quasi-uniformly over the condensate which expands and picks up angular velocity (Fig. 1(c)). Subsequently, over a long period, further vortices leave (and for larger values of α may enter) the dense region, until finally a regular lattice of 12

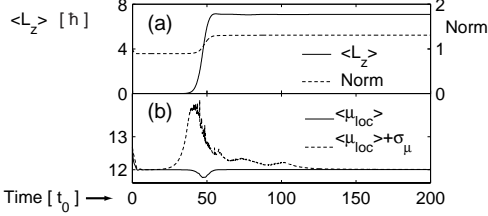


FIG. 2: Time evolution of condensate quantities for the case of Fig. 1. (a) $\langle L_z \rangle$ and norm, (b) $\langle \mu_C \rangle$ and σ_μ (in units of $\hbar\omega$).

vortices rotating at angular velocity α in the lab frame remains (Fig. 1(d)).

The overall time scale of the process is illustrated in Fig. 2(a) which shows the total angular momentum increasing sharply around $t \approx 40$, when the 16 vortices enter the dense part of the condensate. For a given seeding, the timescale for this onset is determined by γ and to good approximation scales as γ^{-1} . The *local chemical potential* $\mu_{loc}(x)$ (defined as the absolute value of the right-hand side of Eq. (1) divided by ψ_R) provides a useful characterisation of the temporal development. In Fig. 2(b), we plot the evolution of the spatial mean of $\mu_{loc}(x)$, which exhibits a rapid initial adjustment (to $\approx \mu$), as the condensate roughly equilibrates with the thermal cloud, and a later dip at $t \approx 48$ during which the number of atoms in the condensate increases (see Fig. 2(a)). The spatial variance σ_μ of $\mu_{loc}(x)$ quantifies the deviation of the solution from equilibrium (where it is zero). It becomes large as the vortices enter the dense region of the condensate, and its subsequent slow decay indicates the long time needed for stabilization of the vortex lattice. It is not easy to characterise the latter time scale, since the local chemical potential can be almost constant everywhere, with possibly only a single vortex not in its final place. From a large number of simulations we have found that the number of vortices in the stable final lattice increases with α and μ , and is generally different from the number seen in the initial ring. It also exhibits a very weak dependence on the exact form of the seeding. For the case of $\mu = 12\hbar\omega$ the critical value for the appearance of any vortices is found from the simulations to be $\alpha = 0.444\omega$, at which speed an irregular ring of 10 vortices appears initially, settling down eventually to three vortices in a lattice inside the Thomas-Fermi radius. Three dimensional simulations of Eq. (3) also confirm the general behavior seen in Fig. 1.

Analytic treatment: An analytic understanding of the nucleation and growth process of the vortices can be obtained from Eq. (3) by considering the linearized Bogolyubov excitations above the initial state, which have angular momentum l and energy eigenvalues $\epsilon_{n,l}$ measured relative to μ_C . From the final term of Eq. (3) we see that excitations for which $\epsilon_{n,l} < \mu - \mu_C + \hbar\alpha l$ will experience a positive growth rate $G \approx \gamma(\mu - \mu_C + \hbar\alpha l - \epsilon_{n,l})/\hbar$. Initially this causes rapid growth of the condensate (the $n = l = 0$ component, which has the lowest eigenvalue) until the condensate and thermal cloud approximately equilibrate ($\mu \approx \mu_C$). Subsequently, the gain of the other components is $\gamma(\epsilon_{n,l}/\hbar - \alpha l)$, and thus the critical value of α for positive gain is given by $\epsilon_{0,l} = \hbar\alpha l$, the

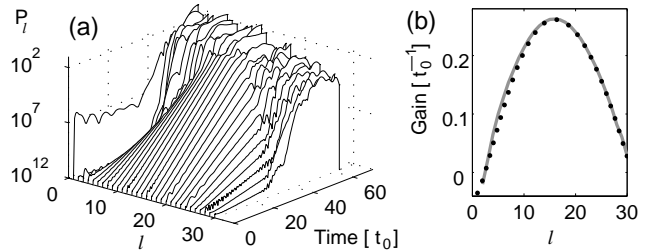


FIG. 3: (a) Evolution of angular momentum occupation probabilities P_l for $l = 1$ to 30 for the case of Fig. 1. (b) Comparison of gain coefficients of l components obtained from the simulation in Fig. 1 (solid line) with the predicted gain coefficients $G = \gamma(\epsilon_{0,l}/\hbar - \alpha l)$ (dotted line).

same condition for criticality found in [19]. Above criticality, the dominant value l_v is that which maximizes the gain, and is given by $\partial(\epsilon_{0,l} - \hbar\alpha l)/\partial l = 0$, and a crude estimate for l_v can be obtained by minimizing $\hbar^2 l^2/2mr^2 - \hbar\alpha l$ at the Thomas-Fermi surface, to give $l_v \approx \pi R_{TF}^2 2m\alpha/\hbar$. This is the number of vortices which would result from filling a disk of radius R_{TF} with a vortex lattice [22]. In the initial stages of vortex formation, when the process is still linear, the wavefunction of the condensate takes the form (for simplicity including only the excitation with maximum gain, which has angular momentum $\hbar l_v$ and energy $\hbar\omega_v \equiv \epsilon_{0,l_v} - \hbar\alpha l_v$)

$$\psi_R \approx e^{-i\mu_C t/\hbar} \left\{ \xi_0 + e^{il_v\phi+Gt} [ue^{i\omega_v t} + ve^{-i\omega_v t}] \right\}. \quad (4)$$

Here $\xi_0(r)$ is the initial rotationally symmetric condensate wavefunction, ϕ is the azimuthal angle, and $u(r), v(r)$ are obtained by solving the Bogolyubov-de Gennes equations. The essential behavior can be seen by neglecting $v(r)$, so that ψ has l_v zeroes—that is vortices—given by the interference of the two terms. These vortices all occur at the same radius, initially at infinity. Since the long distance behavior of $u(r)$ must be less rapid than that of $\xi_0(r)$, the ring will steadily shrink as the excitation grows. The time dependence of the coefficient means that the ring of vortices rotates at the angular frequency ω_v in the rotating frame. In a more detailed picture, more values of l should be included, and the corresponding superposition will be an imperfectly circular ring of vortices, perhaps containing more than l_v vortices.

This analytic treatment can be verified by decomposing the condensate into angular momentum components, and plotting the occupation values P_l against time, as in Fig. 3(a). We see that the l components above threshold grow exponentially up to the time $t \approx 40$ (when the vortex ring passes through the Thomas-Fermi radius), and the gain is maximum for $l_v = 16$. In Fig. 3(b) we compare the gain prediction $\gamma(\epsilon_{0,l}/\hbar - \alpha l)$ (obtained by calculating the surface modes $\epsilon_{0,l}$ for a condensate with $\mu_C = 12\hbar\omega$) against the gain rates measured from the simulation. Not only is our gain prediction very accurate, but we also find that the spatial particle density for each l component very accurately matches the prediction from the corresponding Bogolyubov wavefunction.

Rotating trap, no thermal cloud: Finally, we consider the connection between stirring and growth. As an example of

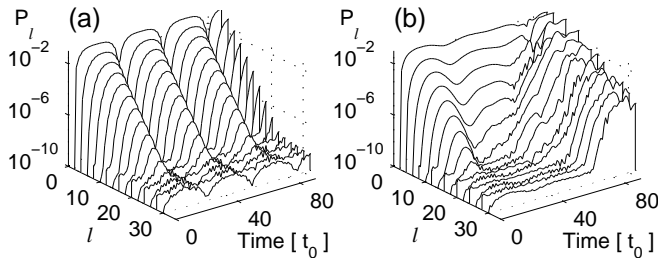


FIG. 4: Evolution of angular momentum occupation probabilities P_l for: (a) rotating elliptical trap with no thermal cloud ($\gamma = 0$); (b) rotating elliptical trap and corotating thermal cloud. Only the even l states are shown. Parameters as in Fig. 1 except trap parameters $\omega_x = 1.05 \omega$, $\omega_y = 1.15 \omega$ and $\alpha = \Omega = 0.65 \omega$.

a case of pure stirring we have simulated a rotating elliptical trap in the absence of a thermal cloud. The general behavior is well represented by the case $\mu_C = 12.5\hbar\omega$ and $\Omega = 0.65\omega$, for which we find that the condensate deforms into an elliptical shape rotating at the trap frequency, and a similarly deformed ring of about 28 vortices shrinks until it meets the dense part of the condensate at its narrowest radius. The resulting state is a distorted version of Fig. 1(b) [23], and this subsequently undergoes an oscillatory behavior, but with no further penetration of the vortices into the condensate. Only the even angular momentum components of the condensate become significantly occupied and undergo periodic cycling (Fig. 4(a)). This can be well understood in terms of the Rabi cycling model [14], noting that an elliptical potential can connect the initial ground state only to states of even l . Resonant mixing to the surface modes will occur when $\epsilon_{0,l} - \hbar\Omega l = 0$, and the lowest value of Ω for which this occurs (when also $\partial(\epsilon_{0,l} - \hbar\Omega l)/\partial l = 0$) gives the same condition for criticality as found in Refs. [11, 12, 13]. This is also exactly the same condition as for the rotating cloud.

Rotating trap with a thermal cloud: Now repeating this simulation, but with a thermal cloud (Eq. (3) with $\alpha = \Omega$ and $\gamma \neq 0$), we get dramatically different results. The same elliptical distortion of the condensate occurs, but the effect tends to smooth out with time. A distorted vortex ring appears, with an initial number of vortices as expected from the growth mechanism (here ≈ 14), and then shrinks into the condensate and nucleates the vortex lattice. The angular momentum projections in Fig. 4(b) show the difference very clearly. The vortex lattice is the result of the growth process, which is essentially superposed on the effects of stirring, eventually masking them. This scenario leads to the conclusion that the principal effect of the rotating trap is to produce a rotating thermal cloud, which then transfers angular momentum into the condensate, eventually forming the vortex lattice.

Comparison with other work: The main point of this paper is the analysis of vortex formation in terms of the growth in occupation of modes with non-zero angular momentum. This requires the presence of a rotating thermal cloud, but stirring the condensate can seed angular momentum components which may then grow from the thermal cloud by stimulated collisions. The critical angular velocity of the thermal cloud to allow growth is the same as the critical angular velocity re-

quired for stirring to resonantly mix surface modes with the condensate, and agrees with the latter values calculated by previous workers [11, 12, 13, 19]. However, our treatment goes beyond the critical point, after which the behavior of the two processes becomes quite different, and includes the full dynamics of lattice stabilization. Our vortex growth equation (3) can be solved without linearization or using hydrodynamic methods, and its solutions can be interpreted in a straightforward quantum mechanical way. The dynamics of the thermal cloud are suppressed in this paper, but their inclusion is necessary for the full understanding of vortex lattice dynamics, including lattice decay, which can also be treated by our formalism.

This work was supported by the Marsden Fund of New Zealand under contract PVT-902.

- [1] A. L. Fetter and A. A. Svidinsky, *J. Phys. Condens. Matter* **13**, R135 (2001).
- [2] D. L. Feder, C. W. Clark, and B. I. Schneider, *Phys. Rev. A* **61**, 011601(R) (1999).
- [3] K. W. Madison, F. Chevy, W. Wohlleben, and J. Dalibard, *Phys. Rev. Lett.* **84**, 806 (2000).
- [4] K. W. Madison, F. Chevy, and J. Dalibard, *Phys. Rev. Lett.* **86**, 4443 (2001).
- [5] P. C. Haljan, I. Coddington, P. Engels, and E. A. Cornell, *Phys. Rev. Lett.* **87**, 210403 (2001).
- [6] C. Raman, J. R. Abo-Shaeer, J. M. Vogels, K. Xu, and W. Ketterle, *Phys. Rev. Lett.* **87**, 210402 (2001).
- [7] J. R. Abo-Shaeer, C. Raman, J. M. Vogels, and W. Ketterle, *Science* **292**, 476 (2001).
- [8] J. R. Abo-Shaeer, C. Raman, and W. Ketterle, *Phys. Rev. Lett.* **88**, 070409 (2002).
- [9] E. Hodby, G. Heckenblaikner, S. A. Hopkins, O. M. Maragó, and C. Foot, *Phys. Rev. Lett.* **88**, 010405 (2001).
- [10] A. L. Fetter, *Phys. Rev. A* **64**, 063608 (2001).
- [11] F. Dalfovo and S. Stringari, *Phys. Rev. A* **63**, 011601 (2000).
- [12] J. R. Anglin, *Phys. Rev. Lett.* **87**, 240401 (2001).
- [13] A. E. Muryshev and P. O. Fedichev, *cond-mat/0106462*.
- [14] B. M. Caradoc-Davies, R. J. Ballagh, and K. Burnett, *Phys. Rev. Lett.* **83**, 895 (1999).
- [15] M. J. Davis and C. W. Gardiner, *J. Phys. B* **35**, 733 (2002).
- [16] C. W. Gardiner, P. Zoller, R. J. Ballagh, and M. J. Davis, *Phys. Rev. Lett.* **79**, 1793 (1997).
- [17] O. N. Zhuravlev, A. E. Muryshev, and P. O. Fedichev, *Phys. Rev. A* **64**, 053601 (2000).
- [18] C. W. Gardiner, J. R. Anglin, and T. I. A. Fudge, *J. Phys. B* **35**, 1555 (2002).
- [19] J. E. Williams, E. Zaremba, B. Jackson, T. Nikuni, and A. Griffin, *Phys. Rev. Lett.* **88**, 070401 (2002).
- [20] D. L. Feder, C. W. Clark, and B. I. Schneider, *Phys. Rev. Lett.* **82**, 4956 (1999).
- [21] M. Tsubota, K. Kasamatsu, and M. Ueda, *Phys. Rev. A* **65**, 023603 (2002).
- [22] R. J. Donnelly, *Quantized vortices in helium II* (Cambridge U. P., Cambridge, 1991).
- [23] MPEG movies showing these results are available from URL <http://www.physics.otago.ac.nz/bec/theory.htm>.